AD

ANALYSIS OF LAUNCH-INDUCED MOTION OF A HYBRID ELECTROMAGNETIC/GAS GUN: INCLUDING EXTENDED FORMULATION OF DOWN-BARREL RECOIL LOADS

E. KATHE
R. GAST
P. VOTTIS
M. CIPOLLO

OCTOBER 1996

19970210 006

DISCLAIMER

The findings in this report are not to be construed as an official Department of the Army position unless so designated by other authorized documents.

The use of trade name(s) and/or manufacturer(s) does not constitute an official indorsement or approval.

DESTRUCTION NOTICE

For classified documents, follow the procedures in DoD 5200.22-M, Industrial Security Manual, Section II-19 or DoD 5200.1-R, Information Security Program Regulation, Chapter IX.

For unclassified, limited documents, destroy by any method that will prevent disclosure of contents or reconstruction of the document.

For unclassified, unlimited documents, destroy when the report is no longer needed. Do not return it to the originator.

REPORT DOCUMENTATION PAGE

1. AGENCY USE ONLY (Leave blank)	2. REPORT DATE October 1996	3. REPORT TYPE AND DATES COVERED Final

4. TITLE AND SUBTITLE
ANALYSIS OF LAUNCH-INDUCED MOTION OF A HYBRID
ELECTROMAGNETIC/GAS GUN: INCLUDING EXTENDED
FORMULATION OF DOWN-BARREL RECOIL LOADS

5. FUNDING NUMBERS
AMCMS No. 6111.01.91A1.1

6. AUTHOR(S)
E. Kathe, R. Gast, P. Vottis, and M. Cipollo

7. PERFORMING ORGANIZATION NAME(S) AND ADDRESS(ES)
U.S. Army ARDEC
Benet Laboratories, AMSTA-AR-CCB-O
Watervliet, NY 12189-4050

8. PERFORMING ORGANIZATION REPORT NUMBER
ARCCB-TR-96030

9. SPONSORING/MONITORING AGENCY NAME(S) AND ADDRESS(ES)
U.S. Army ARDEC
Close Combat Armaments Center
Picatinny Arsenal, NJ 07806-5000

10. SPONSORING/MONITORING AGENCY REPORT NUMBER

11. SUPPLEMENTARY NOTES

12a. DISTRIBUTION/AVAILABILITY STATEMENT
Approved for public release; distribution unlimited.

12b. DISTRIBUTION CODE

13. ABSTRACT (Maximum 200 words)

Great strides have been made in recent years to identify the dominant loads that cause beam-type vibrations of cannons during ballistic operation. These motions infringe upon shot accuracy, because at projectile disengagement, the muzzle's kinematic state may compromise the projectile's intended flight path. This is particularly relevant to coil gun loading, which, unlike gas launch, applies the recoil load to the muzzle end of the barrel instead of the breech. This effectively places the barrel in a state of columnar compression during the launch cycle that may exacerbate structural vibrations known as gun "whip."

14. SUBJECT TERMS
Electromagnetic, Coil, Gun, Dynamics, Accuracy, Recoil

15. NUMBER OF PAGES
20

16. PRICE CODE

17. SECURITY CLASSIFICATION OF REPORT UNCLASSIFIED	18. SECURITY CLASSIFICATION OF THIS PAGE UNCLASSIFIED	19. SECURITY CLASSIFICATION OF ABSTRACT UNCLASSIFIED	20. LIMITATION OF ABSTRACT UL

TABLE OF CONTENTS

LIST OF FIGURES

INTRODUCTION

This paper explores the mathematical relationships between beam vibration and imposed launch loading. Launch loads include forces from down-barrel coil reaction, traditional gas propellent pressures, and projectile-barrel interaction loads. Benét Laboratories' proven Uniform Segments Method (USM) gun vibration model is used to analyze and simulate firing dynamic response of a 60-mm hybrid cannon. The cannon was designed and constructed at Benét Laboratories in collaboration with an electrical engineering group from Polytechnic University at Brooklyn, NY.

BACKGROUND

Great strides have been made in recent years to identify the dominant loads that cause beam-type vibrations in cannons during ballistic operation. These motions infringe upon shot accuracy, because at projectile disengagement, the muzzle's kinematic state may compromise the projectile's intended flight path. In the case of gas guns, the dominant loads that cause these motions have been identified as interactions with the cannon's supports and eccentrically-applied inertia loads due to non-centered masses attached to the barrel (breech, bore evacuator, muzzle brake) or non-symmetric loads due to take-up of slack in support and recoil components. Significant muzzle motions have been modeled [1,2] and reproduced in tests [3] when these conditions exist.

The incorporation of electromagnetic propulsion at the muzzle end of a traditional gas gun invokes a new load on the structure. This loading is manifest as a coaxial reaction force imposed on the muzzle end of the barrel. It may be modeled as a *follower force* that moves with the barrel during vibrational deformation, such that the reaction load is always tangent to the deformed center line of the barrel at the location of the electromagnetic accelerator. This force places the barrel in a state of columnar compression that tends to exacerbate the transverse vibrations of the Gun system during launch. This in turn may lead to an undesirable increase in round-to-round dispersion.

This paper presents a comprehensive model of hybrid gun dynamics that allows computer simulation of various parametric configurations. This will enable the engineer to include design-for-accuracy considerations and provide the opportunity to modify barrel stiffness, axial position of the electromagnetic accelerator, and mount geometry to avoid shot ejection at a time of significant structural deflection.

ANALYSIS AND MODELING OF PROFILE-DEPENDENT LOADS

In this paper the gun vibrations are analyzed from the perspective of transverse beam dynamics. To achieve this, the gross rearward motion of the gun system—due to the rigid-body recoil of the barrel—must be decoupled from its transverse vibrations. In this section, equivalent

1

transverse forcing functions will be developed, and a solution provided based on modal superposition.

Recoil Inertia Load

Recoil is the reaction force placed on the barrel, by Newton's third law, that balances the launch loading imposed on the projectile. The recoil direction of a gun is a function of the mount within which it resides. Current design philosophy specifies that rail and channel sliding surfaces be used in future gas gun designs. This method of support attenuates gun curvature within the mount, maintaining a straight pull that tends to "snap" the overhanging muzzle end of the gun. An inertia couple occurs that is proportional to the slope of the deflection curve and recoil acceleration. This load is expressible for a uniform beam segment as follows: [4]

$$f_r(t,x,y,'y'') = \rho\,\alpha\big[(L-x)y'\big]'$$

(1)

where:

f_r	=		recoil inertia load per unit length
α	=	$\alpha(t)$ =	recoil acceleration
t	=	time	
L	=	length of gun	
x	=	spatial coordinate along bore axis	
y	=	$y_d + y_s$ =	transverse displacement of bore
y_d	=	$y_d(x,t)$ =	dynamic displacement of bore
y_s	=	$y_s(x)$ =	static displacement of bore (caused by gravity droop, manufacture, etc.)
ρ	=	$\rho(x)$ =	linear density of gun
$'$	=	$\partial/\partial x$	

Pressure Curvature Load

Due to the nature of curvature within beam-type structures, diametrically opposite bore surfaces possess differing areas. A pressure load acting within the bore tends to straighten the gun tube because the area of the concave surface is greater than its convex counterpart. This phenomenon is often referred to as the "Bourdon effect." This type of load travels behind the projectile and is proportional to the second derivative of the deflection curve. The expression for this load function is [4]

$$f_c(t,x,y'') = -A_b P_b y'' \big[H(x_p - x)\big]$$

(2)

2

where:

f_c	=	pressure curvature load per unit length
A_b	=	bore area of tube
P_b	=	$P_b(t)$ = propellant gas pressure
$H(x_p - x)$	=	Heaviside unit step function

$$H = 1 \text{ for } 0 < x \leq x_p$$
$$H = 0 \text{ for } x > x_p$$

x_p	=	$x_p(t)$ = axial location of projectile

Projectile Trajectory Load

The accelerating projectile, although considerably less massive than the tube, can exert a significant transverse force when it is constrained to travel along a curved path. This load, which contains transverse, Coriolis, and centrifugal accelerations, is modeled as a point load applied at the instantaneous axial location of the projectile and is expressed as follows:[4]

$$f_p\left(t, x, x_p, \dot{x}_p, y'', \dot{y}', \ddot{y}\right) =$$

$$-m_p\left[\ddot{y} + g + 2\dot{x}_p \dot{y}' + \dot{x}_p^2 y''\right]\delta\left(x_p - x\right)$$

(3)

where:

f_p	=	projectile trajectory load per unit length
g	=	acceleration of gravity
m_p	=	projectile mass
$\delta(x_p - x)$	=	Dirac δ function, in units of length^{-1}

$$\delta(x_p - x) = 0 \text{ for } x \neq x_p$$

$$\int_{-\infty}^{\infty} \delta(x_p - x)dx = 1$$

$\bullet$	=	$\partial/\partial t$

Electromagnetic Load

The reactive loading placed on the barrel by the electromagnetic augmentation of a short stack of coils may be modeled as a *follower force* positioned at the geometric center of the coil stack. As such, this load, which is computed off-line using a finite element method, is oriented along the axis of the coil pack and is subjected to the lateral and angular deflection of the barrel at that point. This force may be resolved into two orthogonal components: parallel to the undeformed center line axis, and perpendicular to the undeformed axis. The perpendicular component may be directly added to the lateral forcing function at the application point. The parallel component pushes the entire gun system forwards or rearwards (a decoupled rigid-body loading) and effects a distributed moment along the length of the barrel (a distributed transverse loading) expressible as: $M(t,x) = f_{em}(t) cos(y'(x)|_{x=xem})[y(x) - y(x)|_{x=xem}]$. In this expression, the

force and cosine terms resolve the parallel component of the time-dependent point electromagnetic loading. The term in the brackets represents the effective lateral moment arm between any point along the barrel and the point of electromagnetic load application at x_{em}. In addition to the distributed moment, the Euler beam reaction to the parallel component effects a lateral point load contribution that cancels the perpendicular component under the small angle approximation. (For elaboration of follower forces, see Reference [5]). Explicit derivation of this load function is explained below. The equivalent lateral load of a distributed moment of the Euler beam is its second spatial derivative.[6] The resulting force is expressed as

$$f_f(t,x) = f_{em}(t)\left[y'' H(x_{em} - x) \right]$$

(4)

where:

f_f	=	equivalent follower force load per unit length
f_{em}	=	electromagnetic follower force (reaction load placed on gun)
x_{em}	=	axial position of electromagnetic follower force

$$|y'| << 1 \text{ for all } 0 \le x \le L$$

It can clearly be seen from this form of the follower force loading that the distributed loading of the barrel is proportional to the curvature at any point along the barrel behind x_{em}. (Loading ahead of x_{em} is indistinguishable from gas recoil loads and is accounted for in equation, (1), which is based on the rigid body acceleration due to all combined launch loads). When the projectile is positively accelerated, the reaction force is negative. Thus, at locations of positive curvature (concave up) the equivalent transverse loading is negative, exacerbating the deflection. The converse is also true; locations of negative curvature are forced upwards. It is clear that *compressive* electromagnetic loading further aggravates locations of greater curvature, behind the accelerator, in the barrel.

TOTAL TRANSIENT SOLUTION

The solution method used in this study is called the "Uniform Segments Method" (USM), which was developed at Benet Laboratories in the mid-1980s.[7] It employs a modal analysis technique in which the gun tube is sectioned into a number of uniform segments within which the Euler-Bernoulli beam equation for free vibration is applied. (For elaboration on Euler-Bernoulli beam equations and modal analysis techniques, see References [8], [9], or [10]). The boundary conditions of the beam are free-free, and intersegment continuity of displacement, slope, bending moment, and shear force is preserved at the interfaces. Each segment possesses a unique mode shape function for each natural frequency. These functions satisfy the continuity requirements cited above and are orthogonal. The terms of these functions contain the usual trigonometric and hyperbolic forms seen in uniform beam analysis. The natural frequencies and coefficients of the terms are solved from the master system matrix formed from the boundary and intersegment

4

continuity conditions. Loads due to support reactions and nonstructural mass (such as the breech) are superimposed with the load formulations of equations (1) through (4) and applied as external loading during the transient solution. They are not accounted for in the modal analysis portion.

Using modal analysis techniques, the dynamic profile of the bore center line may be expressed as the product of two single variable functions, one in space and one in time. This is the *method of separation of variables* in differential equations

$$y_d(t,x) = \sum_{i=1}^{N}\left(\sum_{j=1}^{M}\varphi_{ij}(x)\right)q_i(t) \tag{5}$$

where:

N = number of mode shapes in analysis
M = number of uniform segments in analysis
$\varphi_{ij}(x)$ = mode shape function: j^{th} segment, i^{th} mode
      Note: $\varphi_{ij}(x)$ may only be nonzero for x within the jth segment
$q_i(t)$ = displacement amplification coefficient: i^{th} mode

This method effects a basis transform from the time evolution of an infinite number of transverse displacements, corresponding to the continuum along x, to the time evolution (amplification coefficients) of an infinite number of orthogonal mode shapes. Later in this paper, justification is provided for truncating the number of natural vibration mode shapes to N. This provides the motivation for the basis transform. The advantage of USM over other modal techniques is its piece-wise analytic formulation of the mode shapes, which lends itself to the determination of the curvature-dependent loadings of equations (1) through (4). Standard numerical procedures for modal analysis vibration solutions are used in solving for the amplification coefficients. For a detailed exposition of USM, see Reference [11].

DEVELOPMENT OF HYBRID GUN VIBRATIONAL MODEL

The two main concerns in developing a gun model for use by USM are that:

●   The modal parameters of the model accurately represent the modal parameters of the component.
●   A minimum number of mode shapes be selected to establish model convergence before any reliable calculations are made.

These concerns are addressed below.

5

<u>Establishment of Modal Parameters</u>

To model transverse vibrations of a gun via the modal technique of equation (5) requires an accurate representation of the natural frequencies and mode shapes of the barrel. This entails the selection of the boundary locations, normalized weight, and bending resistance of each segment, such that the free vibration frequencies and mode shapes of the entire model accurately mimic the component. Mode shapes and frequencies determined by a finite element method (FEM) implemented in MATLAB were used to provide a comparative set of modal parameters.[12]

The geometric and model representations of the gun tube are shown in Figure 1. The geometry is simple, because the system was designed for experimental validation. The MATLAB model employed a total of 74 beam elements, whereas the USM model has three segments that were chosen so that the total beam mass was preserved.

FEM Model: 74 Elements

USM Model: 3 Elements
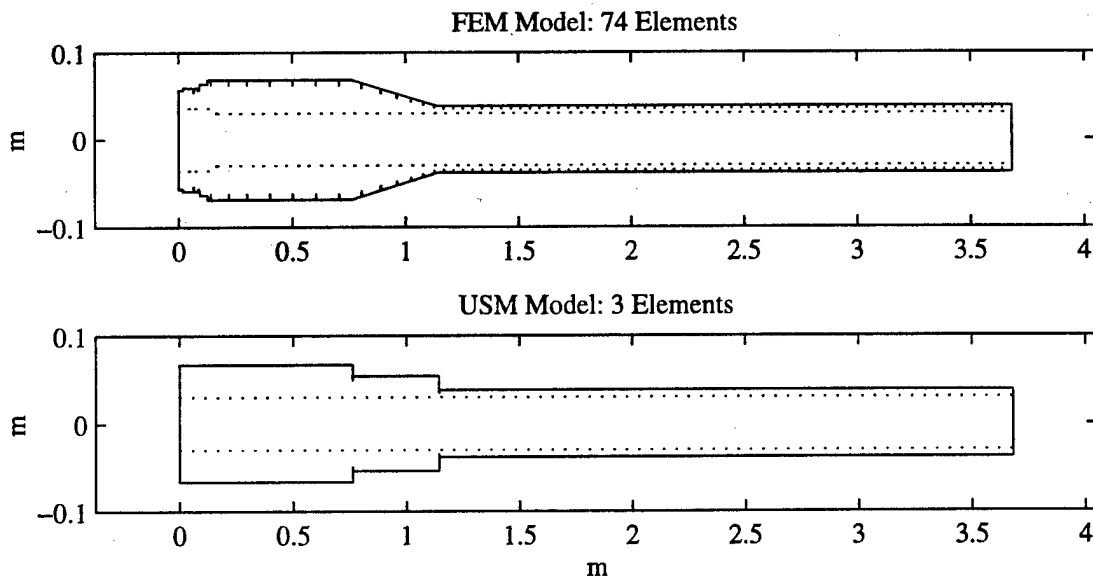
Figure 1. Cylindrical barrel geometry and spatial discretization of FEM and USM models. Hash marks represent nodes between finite elements and uniform segments, respectively.

The first six natural frequencies are shown in Figure 2 along with vibrational mode shapes. The modes match well with an increasing difference in the higher frequencies. In general, the method of modal analysis simplifies the dynamic solution because arguments based on structural damping and mechanical impedance imply that at some —application specific— cut-off frequency, the inclusion of higher modes contributes a negligible amount to the dynamic solution. It has been shown that eight mode shapes (two rigid body, and six flexible) are sufficient to model the 60-mm gun barrel.[13]
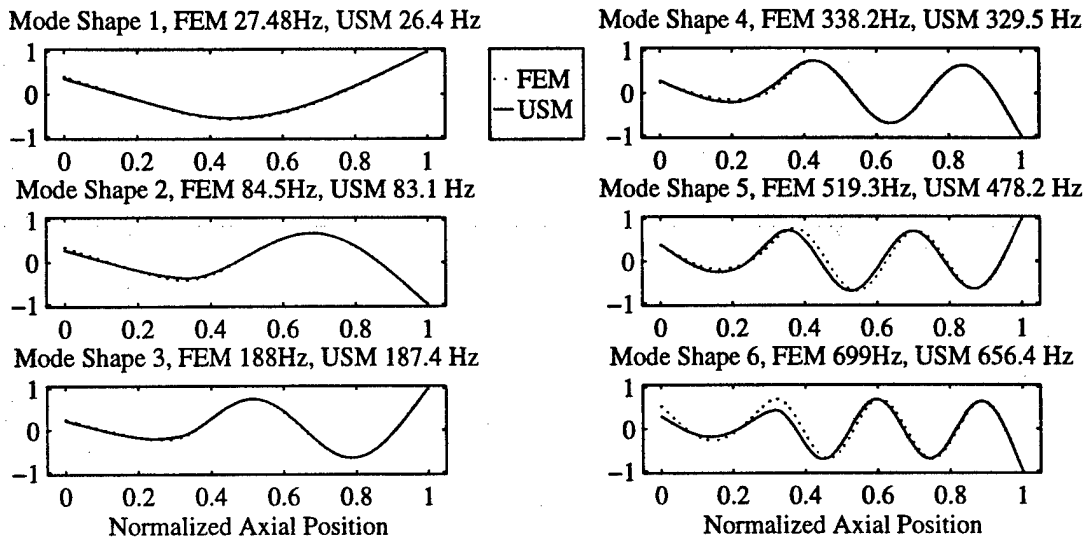
Figure 2. **Mode shape and frequency comparison of the barrel computed using FEM (*dotted line*) and USM (*solid line*). Mode shapes have been unit-normalized in both axial length and transverse deflection.**

RESULTS

The gun dynamic simulation of a hybrid launch was run on the cannon designed and constructed at Benét Laboratories in collaboration with an electrical engineering group from Polytechnic University at Brooklyn, NY.[14] The simulations were conducted for an armature/projectile of mass 412 g, with 46.5 g of IMR4227 propellant. This provides a gas-propelled speed of about 600 m/s. For this simulation, the electromagnetic augmentation was provided by a two-coil accelerator configuration with the coils separated by a distance equal to the width of two coils. (A full configuration for this system consists of 12 coils operating in 3 phases. This two-coil configuration provides for initial testing of one-half of a circuit for a single phase.) The two 6-turn coils were powered by a 150 μF capacitor, with an initial voltage of 5 kV. The electromagnetic force trajectory, shown in Figure 3, was computed using the electromagnetic finite element package, Flux-2D.[15]
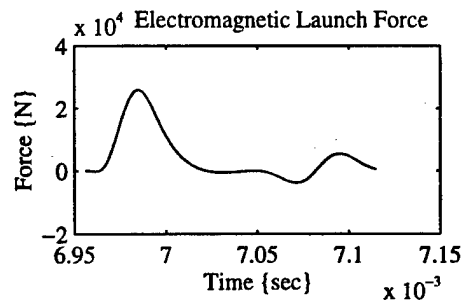
Figure 3. Electromagnetic force applied to the armature/projectile. The force on the barrel is the negative of this.

The dynamic flexure of the hybrid launch is displayed in Figure 4 for three different mounting conditions. As indicated in the title of the subplots, the location of the forward of two hangers is located at three locations: 1.3, 2.5, and 3.7 meters, while the rear hanger is maintained at 0.4 meter. The hangers support the gun system, effecting a simplified gun mount that allows static deflection of the barrel. The plots depict the dynamic muzzle pointing angle. (Note that this does not include the static contribution). Inspection reveals that the deflection oscillates as a function of time, and that the modulation (phase and frequency) of the oscillation may be altered via the parametric changes to the system.

The effect of the electromagnetic loading in these cases may be seen as the discontinuity that occurs near 0.007 second. In the first case, 1.3 meter hanger position, the loading improved the performance of the gun system by giving the muzzle a slight straightening *impulse*. (Although the loading of Figure 3 is not truly impulsive, it is very quick relative to the firing cycle.) In the second case, the same effect is much less pronounced due to the low angular deflection of the muzzle (and the accelerator). In the third case, the loading drove the muzzle further away from its static deflection.

It is desirable to design the system with the least amount of angular deflection at shot ejection to minimize round-to-round dispersion. Achieving this design objective is complicated in practice by the different interior ballistics of various rounds. A design that is *well timed* for one round may be poorly timed for alternate rounds. Thus, a compromised design is sought to reduce variations and sensitivity across a wide range of possible round types.

DOWN-BARREL RECOIL FORMULATION

The purpose of this section is to explicitly derive the transverse beam loading that results from recoil loads that do not necessarily occur at the zero axial position. Such loads may be

8
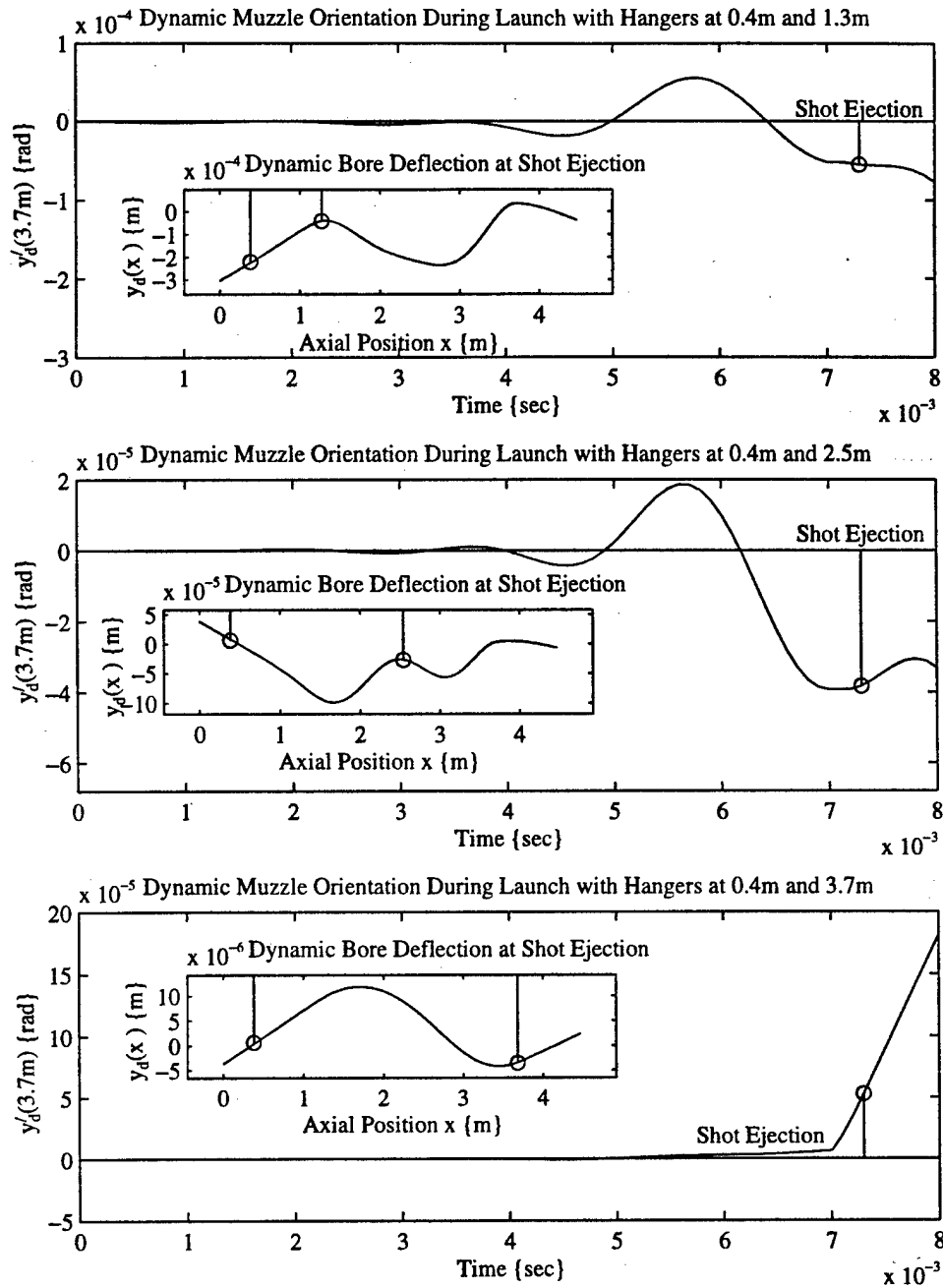
Figure 4. Hybrid gun dynamic simulation for three different system parametric configurations. The three main plots depict the dynamic contribution to the angular deflection of the barrel, at an axial position of 3.7/m, versus time. The insets depict the dynamic contribution to the bore profile at shot ejection.

imposed by down-barrel electromagnetic accelerators. This derivation will develop the method used by Simkins,[4] use the same assumptions/approximations, and extend it to the current application.

The Method of Simkins, Equations (1) through (3)

- ### Development of Simkins Equation 1

  "During the recoil of a gun tube there results an axial load per unit length which is equal to the product of the recoil acceleration, $\alpha(t)$, and the mass per unit length of the tube, $\rho(x)$." This may be interpreted as a distributed D'Alembert inertial force *loading*

$$w(x,t) = -\rho(x)\alpha(t) \tag{6}$$

- ### Development of Simkins Equation 2

  "When the tube is curved, this load creates a moment at any location x, along the tube."

$$M(x,t) = \int_x^L -w(\eta,t)[y(\eta,t) - y(x,t)]d\eta \tag{7}$$

  This integral essentially integrates the distributed D'Alembert loading times the relative lateral moment arm for all points beyond the point of interest, x. One may qualitatively reason that at a given axial position, x, the effect of all barrel inertial beyond x, passes through the barrel at x. Thus the integration from x to L. (This formulation is in agreement with the Extended Hamilton Principle Formulation.)[16]

- ### Development of Simkins Equation 3

  Under the Euler beam assumption that all strain energy is contained within the bending mode, excluding shear and axial strain, the distributed moment of equation (7) may be recast into an equivalent distributed transverse loading. (One that would result in the same distributed moment as equation (7).) This distributed transverse loading is the second spatial derivative of equation (7) under the small angle approximation.

The result obtained is

$$f_r\left(x, y', y'', t\right) = \alpha(t)\left[\rho(x) y'(x,t) - y''(x,t) \int_x^L \rho(\eta, t)\, d\eta\right] \tag{8}$$

Note that this result is equivalent to equation (1) for the uniform mass density within each segment empolyed by the USM. (A slight unit ambiguity exists in the compact notation of equation (1) that is better clarified by equation (8). The integral in equation (8) adds a length unit to the numerator of the second term that is missing in equation (1).)

- **Explicit Derivation**

The double spatial differentiation of equation (7) to determine equation (8) is obtained as follows.

First, invert limits of integration of equation (7), insert equation (6), and separate the two components of the integral

$$M(x,t) = \int_L^x w(\eta, t)\left[y(\eta, t) - y(x,t)\right] d\eta \tag{9a}$$

$$= \int_L^x -\rho(\eta)\alpha(t)\left[y(\eta, t) - y(x,t)\right] d\eta \tag{9b}$$

$$= \alpha(t)\left[y(x,t) \int_L^x \rho(\eta)\, d\eta - \int_L^x \rho(\eta) y(\eta, t)\, d\eta\right] \tag{9c}$$

Second, twice differentiate equation (9c) with respect to x, recalling the chain rule and that the differential of a function under integration—with respect to its upper limit of

11

integration—is the function itself, evaluated at the upper limit

$$M''(x,t) = \alpha(t)\,y(x,t)\rho(x) + \alpha(t)\,y'(x,t)\int_{L}^{x}\rho(\eta)\,d\eta$$
$$-\,\alpha(t)\,y(x,t)\rho(x) \tag{10a}$$

$$M''(x,t) = \alpha(t)\left[y'(x,t)\rho(x) + y''(x,t)\int_{L}^{x}\rho(\eta)\,d\eta\right] \tag{10b}$$

$$M''(x,t) = \alpha(t)\left[y'(x,t)\rho(x) - y''(x,t)\int_{x}^{L}\rho(\eta)\,d\eta\right] \tag{10c}$$

D'Alembert Force Balance

It is important to realize that the spatial integral of $w(x,t)$ along the entire barrel is equal and opposite to the net external axial force placed upon the barrel. For gas launch, this load is solely attributable to the propellant pressure at the breech. (Friction of the projectile and other *high-order* contributions are generally neglected. Also, many modeling techniques, such as in Reference [7], treat extraneous mass attached to the barrel as an external loading.) The D'Alembert force balance may be written

$$\int_{0}^{L}\left(\sum_{d=1}^{K} f_{d}^{AXIAL}(x,t)\right)dx \;-\; \alpha(t)\int_{0}^{L}\rho(x)\,dx = 0 \tag{11a}$$

$$\int_{0}^{L} F_{D}(x,t)\,dx \;-\; \alpha(t)\int_{0}^{L}\rho(x)\,dx = 0 \tag{11b}$$

where:

K	=	number of external axial load sources
$f_{d}^{AXIAL}(x,t)$	=	distributed axial loading for the dth load source
$F_{D}(x,t)$	=	total distributed external loading

12

Gas Launch Contribution

The gas launch contribution, neglecting minor bore diameter variations within the chamber, may be listed as

$$f_1^{\parallel}(t) = -P(t)A_b \cos\left(y'(x,t)\Big|_{x=0} \right) \delta(x-0) \tag{12a}$$

$$f_1^{\perp}(t) = -P(t)A_b \sin\left(y'(x,t)\Big|_{x=0} \right) \delta(x-0) \tag{12b}$$

The first term, the—cosine—component, is the force that is parrallel to the undeformed axis. The perpendicular—sine—component may be directly included in the transverse loading.

Down Barrel Axial Loading

The down barrel electromagnetic follower force may be expressed in the context of equation (11) as

$$f_2^{\parallel}(t) = f_{em}(t) \cos\left(y'(x,t)\Big|_{x=x_{em}} \right) \delta(x-x_{em}) \tag{13a}$$

$$f_2^{\perp}(t) = f_{em}(t) \sin\left(y'(x,t)\Big|_{x=x_{em}} \right) \delta(x-x_{em}) \tag{13b}$$

(Again, the perpendicular—sine—contribution must be directly incorporated into the transverse loading.)

13

Distributed Moment Due to Axial Loading

In analogy with equations (7) and (10), the external axial loads generate distributed moments along the deformed barrel expressible as

$$M(x,t) = \int_{x}^{L} -F_D(\eta,t)[y(\eta,t) - y(x,t)]\,d\eta \qquad (14a)$$

$$M''(x,t) = y'(x,t)\left(-F_D(x,t)\right) - y''(x,t)\int_{x}^{L}\left(-F_D(\eta,t)\right)d\eta \qquad (14b)$$

Distributed Lateral Loading Due to External Axial Loads

Equation (14b) represents the equivalent distributed transverse loading of all combined external axial loads. In both of the loads, equations (12) and (13), the unity integration property of the Dirac δ function is used to compute the second term of equation (14b). Also note that the incoporation of a truely distributed axial loading—such as would be obtained by a long *traveling wave* multi-coil accelerator stack—is directly enabled by equation (14b).

● Lateral Loading Due to Gas Launch

The effective lateral loading due to the pressure at the breech may be expressed as the combination of equation (12b) and the second spatial derivative of the moment created by equation (12a) as shown in equation (14b)

$$f_1(x,t) = -P(t)A_b \sin\left(y'(x,t)\Big|_{x=0}\right)\delta(x-0)$$

$$+ y'(x,t)\left(-\left[-P(t)A_b\cos\left(y'(x,t)\Big|_{x=0}\right)\delta(x-0)\right]\right)$$

$$- y'''(x,t)\int_{x}^{L}\left(-\left[-P(t)A_b\cos\left(y'(\eta,t)\Big|_{\eta=0}\right)\delta(\eta-0)\right]\right)d\eta \qquad (15)$$

In this expression, the first term is the direct perpendicular component of the breech force, equation (12b). The second term cancels the first under the small angle approximation. The third term only has a non-zero value at x = 0. By the definition of the Dirac function, the integral has the value of the function within it at η = x = 0.

14

However, the resultant force distribution is finite over an infinitesimal length—a null function; further the boundary condition of the free end of a beam imposes zero curvature at x = 0. Thus the entire expression of equation (15) contributes negligibly to the gun dynamics solution. (Note: small angle assumptions are intermixed with the Euler beam approximations. Perturbation and stability analysis would require a detailed tracking of all assumptions to prevent confusion with order approximations.)

● Lateral Loading Due To Electromagnetic Launch

The effective lateral loading due to the electromagnetic accelerator may be expressed as

$$
\begin{aligned}
f_2(x,t) = & f_{em}(t) \sin\left(y'(x,t)\Big|_{x=x_{em}} \right) \delta\left(x - x_{em}\right) \\
& + y'(x,t)\left(-\left[f_{em}(t) \cos\left(y'(x,t)\Big|_{x=0} \right) \delta\left(x - x_{em}\right) \right] \right) \\
& - y''(x,t) \int_x^L \left(-\left[f_{em}(t) \cos\left(y'(\eta,t)\Big|_{\eta=x_{em}} \right) \delta\left(\eta - x_{em}\right) \right] \right) d\eta
\end{aligned}
\tag{16}
$$

As in the previous case, the first two terms cancel under the small angle approximation. However, the third term effects a lateral loading as long as x_{em} resides within the limits of integration; this may be seen to result in the Heaviside function. This, combined with the sign cancellation and small angle approximation for the cosine term results in equation (4).

The appearance of the Heaviside function may create confusion when the electromagnetic accelerator is decelerating a round. (This may be done to tune the velocity of a round, or may occur during normal operation as can be seen in Figure 3 near 7.08 seconds.) The confusion arises due to the reversal of the problem; the affect is to compress the barrel between the axial location of the accelerator and the muzzle. Since the Heaviside is zero in that region, it seems as though the expression does not properly address this mode.

The confusion is eliminated by realizing that the electromagnetic contribution to the gross acceleration of the entire barrel is included within the recoil inertia load of equations (1) and (8). In fact, as can be seen in equation (11b), the external axial loads and D'Alembert inertial load could be combined prior to taking the second spatial derivative of the effected moment in equations (8), (10), and (14). Equation (4) may be thought of as *undoing* the transverse inertial loading component that is attributable to the accelerator force, between the breech and accelerator, when in the decelerating mode of operation.

15

CONCLUSIONS

The method presented in this paper will address accuracy considerations early in the design of electromagnetically augmented gun systems. Simulation data may be used to parametrically optimize the design of the gun system from a structural dynamics perspective. This is particularly relevant for hybrid gun systems. Unlike gas propulsion, whose recoil force is manifest at the breech, pulling the inertia of the gun barrel, hybrid electromagnetic recoil forces are located near the muzzle, pushing the inertia of the barrel. This may exacerbate the affect of gun whip but can largely be avoided by altering the system parameters to time the augmenting force to coincide with low-vibration amplitudes of the fundamental modes of the barrel.

REFERENCES

1. Erline, T. F. and Kregel, M. D., "Modelling Gun Dynamics with Dominant Loads," in Proceedings of the Fifth U. S. Army Symposium on Gun Dynamics, ARCCB-SP-87023, Benet Laboratories, Watervliet, NY, 23-25 September 1987.

2. Gast, R. G., "Analytical Comparison of the Accuracy of Tank Weapons," ARDEC Technical Report ARCCB- TR-89023, Benet Laboratories, Watervliet, NY, September 1989.

3. Schmidt, E., "Jump from the M1A1 Tank," BRL IMR 868, Ballistic Research Laboratory, Aberdeen Proving Ground, MD, 1987.

4. Simkins, T. E., "Transverse Response of Gun Tubes to Curvature Induced Load Functions," in Proceedings of the Second U. S. Army Symposium on Gun Dynamics, ARLCB-SP-78013, Benet Weapons Laboratory, Watervliet, NY, 19-22 September 1978.

5. Leipholz, H., *Direct Variational Methods and Eigenvalue Problems in Engineering*, Noordhoff International Publishing, Leyden, The Netherlands, 1977.

6. Beer, F. P. and Johnston, Jr., E. R., *Mechanics of Materials*, McGraw-Hill, Inc., New York, NY, 1981.

7. Gast, R. G., "Normal Modes Analysis of Gun Vibration by the Uniform Segment Method," ARDEC Technical Report ARCCB-TR-87033, Benet Laboratories, Watervliet, NY, November 1987.

8. Meirovitch, L., *Elements of Vibration Analysis*, McGraw-Hill, Inc., New York, NY, 1986.

9. Thompson, W. T., *Theory of Vibration with Applications*, Prentice Hall, Englewood Cliffs, NJ, 1993.

10. Junkins, J. L. and Kim, Y., *Introduction to Dynamics and Control of Flexible Structures*, American Institute of Aeronautics and Astronautics, Inc., Washington, DC, 1993.

11. Gast, R. G., *Modal Analysis of the Dynamic Flexure in Tank Weapons by the Uniform Segments Method*, Ph.D. Thesis, Rensselaer Polytechnic Institute, Troy, NY, 1988.

12. Kathe, E., "MATLAB Modeling of Non-Uniform Beams Using the Finite Element Method for Dynamic Design and Analysis," ARDEC Technical Report ARCCB-TR-96010, Benet Laboratories, Watervliet, NY, April 1996.

13. Gast, R. G., "Curvature-Induced Motions of 60-mm Guns," ARDEC Technical Report ARCCB-TR-94002, Benet Laboratories, Watervliet, NY, January 1994.

17

REFERENCES (Continued)

14. Zabar, Z., Levi, E., and Birenbaum, L., and Vottis, P. M., Cipollo, M., and Kathe, E., "Pulsed Power to the Aid of Chemical Guns," Tenth IEEE International Pulsed Power Conference, Paper 5-3, Albuquerque, NM, 10-13 July 1995.

15. Magsoft Corporation, Flux 2D, Version 7.11: User's Guide, Troy, NY, April 1995.

16. Meirovitch, L., *Analytical Methods In Vibrations,* MacMillan, New York, 1967, pp. 440-443.

TECHNICAL REPORT INTERNAL DISTRIBUTION LIST

	NO. OF COPIES
CHIEF, DEVELOPMENT ENGINEERING DIVISION	
ATTN: AMSTA-AR-CCB-DA	1
-DB	1
-DC	1
-DD	1
-DE	1
CHIEF, ENGINEERING DIVISION	
ATTN: AMSTA-AR-CCB-E	1
-EA	1
-EB	1
-EC	1
CHIEF, TECHNOLOGY DIVISION	
ATTN: AMSTA-AR-CCB-T	2
-TA	1
-TB	1
-TC	1
TECHNICAL LIBRARY	
ATTN: AMSTA-AR-CCB-O	5
TECHNICAL PUBLICATIONS & EDITING SECTION	
ATTN: AMSTA-AR-CCB-O	3
OPERATIONS DIRECTORATE	
ATTN: SIOWV-ODP-P	1
DIRECTOR, PROCUREMENT & CONTRACTING DIRECTORATE	
ATTN: SIOWV-PP	1
DIRECTOR, PRODUCT ASSURANCE & TEST DIRECTORATE	
ATTN: SIOWV-QA	1

NOTE: PLEASE NOTIFY DIRECTOR, BENÉT LABORATORIES, ATTN: AMSTA-AR-CCB-O OF ADDRESS CHANGES.

TECHNICAL REPORT EXTERNAL DISTRIBUTION LIST

	NO. OF COPIES		NO. OF COPIES
ASST SEC OF THE ARMY RESEARCH AND DEVELOPMENT ATTN: DEPT FOR SCI AND TECH THE PENTAGON WASHINGTON, D.C. 20310-0103	1	COMMANDER ROCK ISLAND ARSENAL ATTN: SMCRI-SEM ROCK ISLAND, IL 61299-5001	1
DEFENSE TECHNICAL INFO CENTER ATTN: DTIC-OCP (ACQUISITIONS) 8725 JOHN J. KINGMAN ROAD STE 0944 FT. BELVOIR, VA 22060-6218	2	MIAC/CINDAS PURDUE UNIVERSITY 2595 YEAGER ROAD WEST LAFAYETTE, IN 47906-1398	1
COMMANDER U.S. ARMY ARDEC ATTN: AMSTA-AR-AEE, BLDG. 3022 AMSTA-AR-AES, BLDG. 321 AMSTA-AR-AET-O, BLDG. 183 AMSTA-AR-FSA, BLDG. 354 AMSTA-AR-FSM-E AMSTA-AR-FSS-D, BLDG. 94 AMSTA-AR-IMC, BLDG. 59 PICATINNY ARSENAL, NJ 07806-5000	1 1 1 1 1 1 2	COMMANDER U.S. ARMY TANK-AUTMV R&D COMMAND ATTN: AMSTA-DDL (TECH LIBRARY) WARREN, MI 48397-5000	1
DIRECTOR U.S. ARMY RESEARCH LABORATORY ATTN: AMSRL-DD-T, BLDG. 305 ABERDEEN PROVING GROUND, MD 21005-5066	1	COMMANDER U.S. MILITARY ACADEMY ATTN: DEPARTMENT OF MECHANICS WEST POINT, NY 10966-1792	1
DIRECTOR U.S. ARMY RESEARCH LABORATORY ATTN: AMSRL-WT-PD (DR. B. BURNS) ABERDEEN PROVING GROUND, MD 21005-5066	1	U.S. ARMY MISSILE COMMAND REDSTONE SCIENTIFIC INFO CENTER ATTN: AMSMI-RD-CS-R/DOCUMENTS BLDG. 4484 REDSTONE ARSENAL, AL 35898-5241	2
DIRECTOR U.S. MATERIEL SYSTEMS ANALYSIS ACTV ATTN: AMXSY-MP ABERDEEN PROVING GROUND, MD 21005-5071	1	COMMANDER U.S. ARMY FOREIGN SCI & TECH CENTER ATTN: DRXST-SD 220 7TH STREET, N.E. CHARLOTTESVILLE, VA 22901	1
		COMMANDER U.S. ARMY LABCOM, ISA ATTN: SLCIS-IM-TL 2800 POWER MILL ROAD ADELPHI, MD 20783-1145	1

NOTE: PLEASE NOTIFY COMMANDER, ARMAMENT RESEARCH, DEVELOPMENT, AND ENGINEERING CENTER,
BENÉT LABORATORIES, CCAC, U.S. ARMY TANK-AUTOMOTIVE AND ARMAMENTS COMMAND,
AMSTA-AR-CCB-O, WATERVLIET, NY 12189-4050 OF ADDRESS CHANGES.

	NO. OF COPIES		NO. OF COPIES
COMMANDER U.S. ARMY RESEARCH OFFICE ATTN: CHIEF, IPO P.O. BOX 12211 RESEARCH TRIANGLE PARK, NC 27709-2211	1	WRIGHT LABORATORY ARMAMENT DIRECTORATE ATTN: WL/MNM EGLIN AFB, FL 32542-6810	1
DIRECTOR U.S. NAVAL RESEARCH LABORATORY ATTN: MATERIALS SCI & TECH DIV WASHINGTON, D.C. 20375	1	WRIGHT LABORATORY ARMAMENT DIRECTORATE ATTN: WL/MNMF EGLIN AFB, FL 32542-6810	1

NOTE: PLEASE NOTIFY COMMANDER, ARMAMENT RESEARCH, DEVELOPMENT, AND ENGINEERING CENTER, BENÉT LABORATORIES, CCAC, U.S. ARMY TANK-AUTOMOTIVE AND ARMAMENTS COMMAND, AMSTA-AR-CCB-O, WATERVLIET, NY 12189-4050 OF ADDRESS CHANGES.